RESEARCH ARTICLE | MAY 05 2025

Flexible internal transporter with gravity-assisted mechanism for vertical transfer of microscope head

Angela M. Coe ; Guohong Li ; Eva Y. Andrei

Rev. Sci. Instrum. 96, 053701 (2025)
https://doi.org/10.1063/5.0264135

Review of
Scientific Instruments

ARTICLE

pubs.aip.org/aip/rsi

Flexible internal transporter with gravity-assisted mechanism for vertical transfer of microscope head

Cite as: Rev. Sci. Instrum. 96, 053701 (2025); doi: 10.1063/5.0264135
Submitted: 8 February 2025 • Accepted: 11 April 2025 •
Published Online: 5 May 2025

Angela M. Coe, Guohong Li, and Eva Y. Andrei[a)]

AFFILIATIONS

Department of Physics and Astronomy, Rutgers, the State University of New Jersey, Piscataway, New Jersey 08854, USA

[a)] **Author to whom correspondence should be addressed:** eandrei@physics.rutgers.edu

ABSTRACT

We present a flexible mechanism for vertically transferring scanning probe microscope (SPM) heads in ultra-high vacuum. The microscope head is transferred from a room temperature site down to an SPM pluggable connector at low temperatures within the bore of a superconducting magnet located in a top-loading cryostat. Insertion and extraction of the microscope head to and from the connector are accomplished with gravity-assisted tools. Contrasted with typical rigid designs, the low-profile mechanism described here has no external mounting structure, which reduces sensitivity to mechanical disturbances, decreases vacuum volume, and enables installation in standard laboratory spaces.

I. INTRODUCTION

Advances in scanning tunneling microscopy (STM)[1–3] and spectroscopy (STS) have made it possible to gain insights into the nature of exotic emergent quantum states at low temperatures (LT) in magnetic fields.[4–10] While taking measurements, the STM head is positioned in the center of a superconducting magnet at the bottom of a cryostat. The absence of optical access and the limited working space inside the magnet bore hinder the *in situ* exchange of STM tips and samples as well as their alignment relative to each other. Thus far, the methods that have been developed to handle these challenges invariably utilize an externally mounted rigid vertical transfer mechanism, which imposes stringent requirements as briefly described below.

Dip-stick method [Fig. 1(a)]: The STM is attached to the end of a dip-stick,[11] as is typically done for electrical transport measurements. In this configuration, the STM is loaded with tip and sample in ambient conditions before being lowered into the cryostat. The dip-stick provides rigid mechanical support and electrical wiring to the STM.

UHV top-loader method [Fig. 1(b)]: To study surface-sensitive samples[12,13] and perform *in situ* tip and sample conditioning, the STM head is attached to a support structure on a translation stage within an ultra-high vacuum (UHV) chamber, which is coupled to a top-loading cryostat.[14–16] Tip and sample exchange and alignment are performed at room temperature (RT) in UHV with optical access before the STM is lowered into the cryostat. The translation stage and support structure are tall (>2 m) since their rigid structure must be at least twice the depth of the cryostat, thus limiting use to high-ceilinged laboratories or those with a pit in the floor or, even in some cases, those spanning two floors of a building. Furthermore, attaching tall stages to a UHV system requires long bellows and creates a large volume of dead space, increasing pump-down time. Tall structures pose a challenge to achieving good alignment between the translation axis and the cryostat, requiring support structures and translation stages to control the vertical movement. They are susceptible to picking up vibrations and acoustic noise, anathema to highly sensitive microscopy techniques.

UHV bottom-loader method [Fig. 1(c)]: To reduce the long travel distance imposed by the top-loading configuration, a bottom-loading version was developed.[17–19] Here, the UHV chamber is located below the cryostat, and the STM with its support structure is raised into the magnet. This has the advantage of shortening the travel distance of the STM, which decreases the volume of dead space. However, this requires a more complex and expensive cryostat and a sophisticated UHV chamber design with multilayer

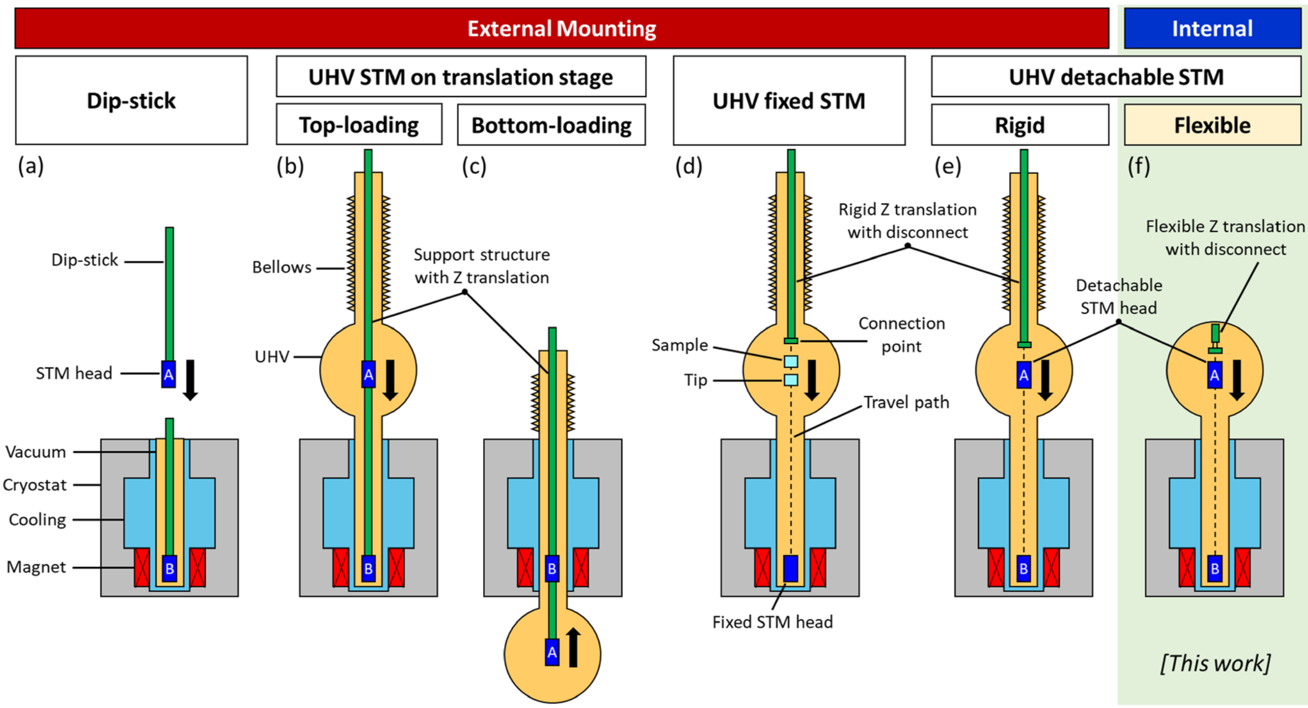

FIG. 1. Methods of vertically transferring STM heads into a superconducting magnet. The magnet is depicted in red, the STM head is blue, the method of transfer is in green, and vacuum or UHV is in orange. The STM is shown in two positions marked "A" and "B," where "A" corresponds to the position for tip and sample exchange and "B" is the position in the magnet for LT measurements. Cartoon schematics are not drawn to scale. (a) Dip-stick method. STM and dip-stick are manually lowered into cryostat and remain connected during measurements. (b) and (c) UHV STM on translation stage methods with (b) a top-loading configuration and (c) a bottom-loading configuration. STM and translation stage remain connected within UHV. Vacuum compatible Z translation is provided to the support structure for vertical travel. (d) UHV with stationary STM head fixed within the cryostat. Tip and sample are transferred to the STM head. Z translation mechanism is rigid and able to disconnect from the sample and tip. Dashed line indicates the path of travel. (e) and (f) UHV detachable STM with (e) a rigid and (f) a flexible Z translation mechanism that can disconnect from the STM head. The flexible mechanism requires no additional vacuum volume since the mechanism is fully contained in the UHV chamber.

thermal shields. In addition, the high center of gravity poses vibration isolation challenges.

UHV fixed STM method [Fig. 1(d)]: To achieve lower base temperatures, the STM is fixed within the magnet and the tip/sample are transferred to the STM.[20–23] A stationary STM facilitates a stronger thermal link between the STM and cooling stage, beneficial for experiments below 300 mK. The smaller size of the tip and sample simplifies the transfer structure and reduces its size. Transfer of the tip and sample into the STM is achieved by pairing the translation stage with a rotation stage and/or a pushrod, which allows for the transfer mechanism to be disconnected and removed during the experiment. This configuration is suitable for studying bulk crystals or thin film samples, but it does not have optical access to allow for precise tip and sample alignment, which is critical for the study of micrometer-sized samples.

Detachable STM with rigid top-loader method [Fig. 1(e)]: Detachable STM heads[24–29] have been developed with pluggable electrical connections, permitting them to be transferable and operated at multiple sites within a system. This allows the STM head to be available for tip and sample exchange and alignment with optical access at RT in UHV before being vertically transferred into the cryostat, enabling the study of micrometer-sized sample devices.[30] Once the STM head reaches the magnet location, it is plugged into an electrical connector, and the rigid vertical transfer arm is disconnected from the STM head.

To overcome the limitations of the externally mounted rigid methods, we developed a novel internally mounted flexible transfer mechanism,[31–33] [Fig. 1(f)], for controlling the vertical movement of a detachable STM head. The design utilizes a winch-based pulley with a unique automated gravity-assisted attachment method to engage and disengage with the STM head. The transporter enables the study of micrometer-sized samples while being fully contained within the UHV chamber, eliminating the need for excess pumping volume. The collapsible component of the pulley reduces its susceptibility to vibrational noise and reduces the size of the transfer mechanism, enabling its use in standard laboratories. Unlike the tall rigid structures, where misalignment is amplified at the target position, the flexible structure has more tolerance providing a local guide to simplify the alignment of the transporter within the cryostat. The structure was successfully implemented into a cryogen-free UHV STM system with base temperatures down to 4 K and magnetic fields up to 9 T.[34,46]

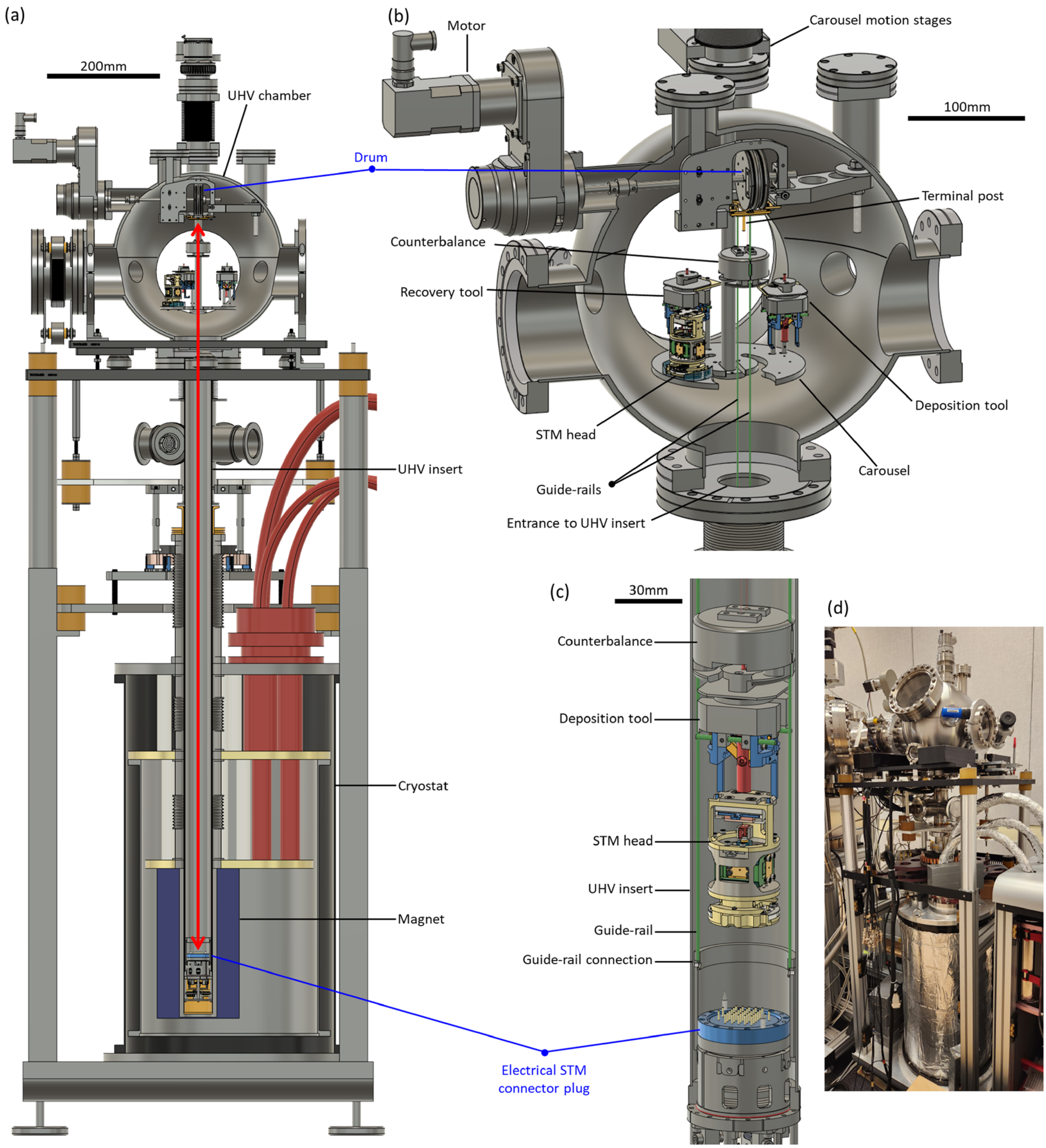

FIG. 2. Overview of transfer assembly. Each schematic is shown with a cross-sectional view of the vacuum chamber, UHV insert, and cryostat. (a) Schematic of vacuum chamber and UHV insert assembly shown installed in a top-loading cryogen-free cryostat. The red arrow indicates the vertical travel path. (b) Vacuum chamber setup depicting winch-based pulley mechanism and the carousel holding the STM head and deposition and recovery tools. (c) Bottom of the UHV insert displaying the STM electrical connector plug located at LT. The magnet and cryocooler are removed for clarity. The counterbalance, deposition tool, and STM head are illustrated en route to the connector plug. (d) Photograph of the outside of the assembly showing the vacuum chamber, UHV insert, and cryostat.

II. DESIGN CONCEPT

The detachable STM head utilized here is a compact, modular quick-connect STM (height 55.5 mm and max diameter of 36 mm) with a pluggable electrical connection at its base. Its full details and performance are previously published.[24,25,34] The goal is to vertically transfer the STM head from a RT-UHV chamber[35] down to a LT STM connector plug located within a magnet, Fig. 2. Once the STM head is plugged in at LT, the transfer mechanism is disconnected from the STM to return to RT while the STM remains at LT. When experiments are concluded, the transfer mechanism is reconnected to the STM at LT and it then returns the STM to RT for tip and sample exchange.

The travel path of the STM head [1.3 m long and indicated as a red arrow in Fig. 2(a)] is within a UHV insert[36] (inner diameter 45.8 mm and length 1.1 m). The bottom of the chamber is attached to the top of the UHV insert. The STM connector plug is mounted to the bottom of the UHV insert and sits in the bore of a superconducting magnet[37] (inner diameter 65.97 mm) located in the belly of a top-loading cryogen-free cryostat[38] with no optical access.[34]

The transfer mechanism[31–33] attaches to the top of the STM via two types of tools: (1) a deposition tool to move the STM head to LT, plug it in, and disconnect from it; and (2) a recovery tool to connect to the STM at LT and return it to RT. The vertical movement of the tools is managed by a winch-based design comprised of a motor-controlled pulley drum housed inside the chamber, Fig. 2(b). Flexible wires wrapping about the pulley drum are attached to a counterbalance, which, when the drum rotates, moves vertically along the travel path on guide rails to the LT connector plug [Fig. 2(c)]. The bottom of the counterbalance has a built-in tool selector that permits attachment to a tool. When not in use, the STM and two tools are stored on a carousel located within the chamber.

In the following sections, we describe details of the transfer mechanism including, how the tools engage and disengage with the STM head using a gravity-assisted mechanism; how the transfer mechanism applies sufficient force to plug in the STM at LT; how the tools interface with the tool selector of the counterbalance; and the construction of the winch-based design.

III. LOW-FORCE ELECTRICAL CONNECTION AND GRAVITY-ASSISTED TOOLS

There are two critical challenges to utilizing a flexible mechanism. The first is that the flexible components can only apply a weak force to plug in the STM head at LT. This contrasts with rigid designs where large forces can be applied through the transfer arm. It is thus vital to develop a method to reliably insert the STM head into the electrical connector plug with the weak force. The second challenge is how to connect and disconnect the transfer mechanism from

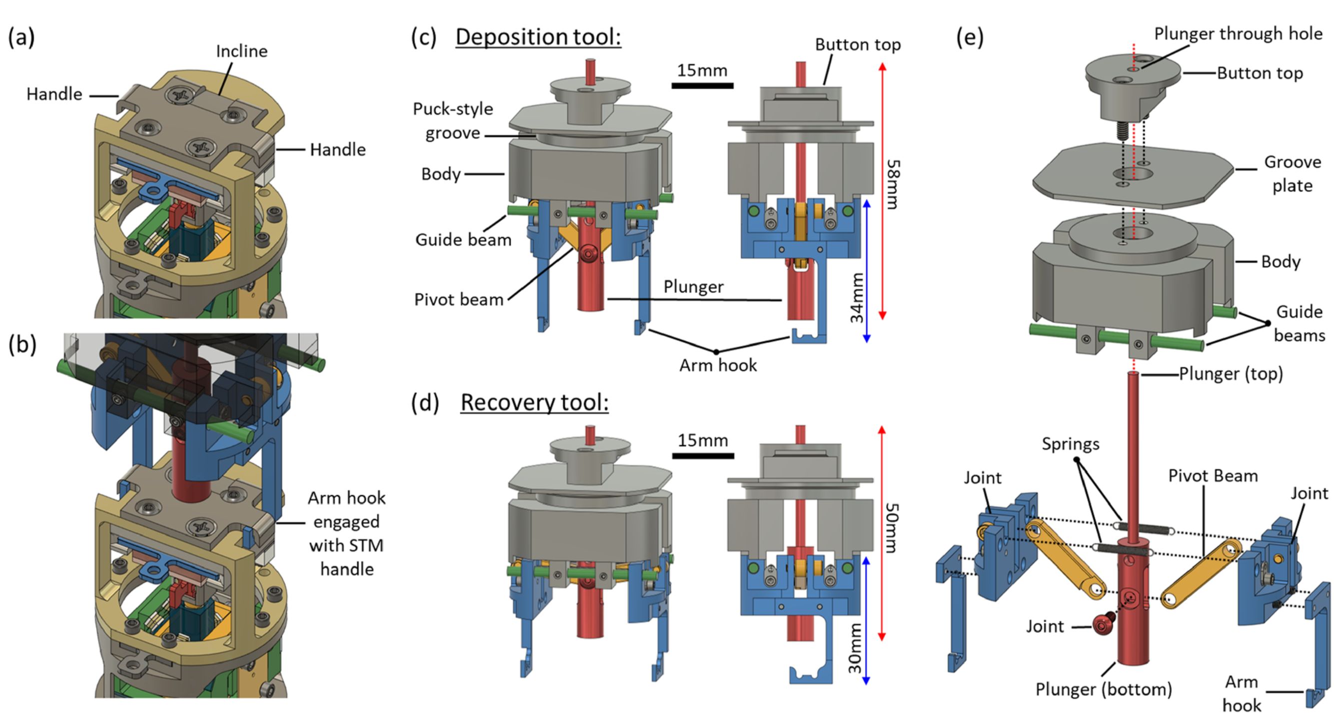

FIG. 3. STM head top plate and deposition and recovery tools. (a) STM head top transfer plate for attaching to the tools. (b) Deposition tool arms/hooks engaged with STM head transfer plate handles. Recovery tool attachment is not shown because it is similar to the deposition tool. (c) Deposition tool from a front and side view. The plunger is indicated in red, the hook arms are depicted in blue, and the pivot beams connecting the plunger and arms are in yellow. Guide beams (green) confine the arm movement. (d) Recovery tool from a front and side view. (e) Exploded view of deposition tool. An exploded view of the recovery tool is not shown because it shares many similarities with the deposition tool.

the STM head. With flexible components, we cannot rely on external mechanisms available in rigid designs, such as rotation stages or pushrods. To address these challenges, we created a low-force electrical connector plug and gravity-assisted tools.

A. Low-force electrical connection

The low-force electrical connector consists of an electrical socket at the bottom of the STM head and the universal electrical plug mounted at the LT site, Fig. 2(c).[24,25] The socket comprises spring-finger contacts[39] that interact with the plug pins[40] to form the electrical connection. This spring-pin interaction is weak, and the total force to insert the STM head (92 g) into the connector plug is 300 g-f (0.29 N) applied to the top of the STM head by the weight of the tool and counterbalance of the transfer mechanism.

The gravity-assisted tools interact with a transfer plate mounted to the top of the STM head [Figs. 3(a) and 3(b)]. The top of the transfer plate is flat to provide a stable surface for the tool to push on and thus plug in the STM head. The transfer plate has two L-shaped handles on either side for interlocking with two hook shaped arms that hang below the body of the tool. An incline at the back of the transfer plate assists with tool attachment to the STM head when in the vacuum chamber.

B. Gravity-assisted tools: Connecting to the STM head

Because a flexible pulley structure is used to provide the vertical travel, an automated triggering mechanism was developed to control the tool arm attachment and detachment to and from the STM head. Both the deposition and recovery tools are designed to convert a vertical movement to a horizontal movement by utilizing gravity to overcome the force of a spring to trigger the action.

The tool engages with the STM via two hook-shaped arms, shown in blue in Figs. 3(c)–3(e). The movement of the two arms on each tool is restricted along a horizontal path by rods.[41] The arms are connected by two compression springs. The horizontal movement of the arms is controlled by the vertical movement of a plunger, indicated in red in Figs. 3(c)–3(e). The plunger, at the center of the tool, is guided along a vertical path and connected to the arms via pivot beams (shown in yellow) with rotating joints. The compression springs provide a resistance force that holds the arms and plunger at one of two fixed positions: either the tool plunger held down or up. The deposition and recovery tools have different arm movements for a given plunger position, providing their distinct depositing and retrieving actions to the STM head. In the case of the deposition tool [Fig. 4(a)], if the plunger is down, then the arms are close together (closed) to hold the STM head. And if the plunger is up, the arms move away from each other (open) to release the STM head. The recovery tool has opposite arm movements [Fig. 4(b)]; the arms are open when the plunger is down and the arms are closed when the plunger is up to engage with the STM head. Further detail on how the tools have opposite arm actions is covered in the Appendix.

Triggering the tool to a different position requires overcoming the compression spring force. The spring force was selected such that the gravitational weight of the tool and counterbalance can overcome the springs so as to trigger the motion of the plunger and arms. The weight of the tool is provided by its body structure [made of 304 stainless steel (SS)].

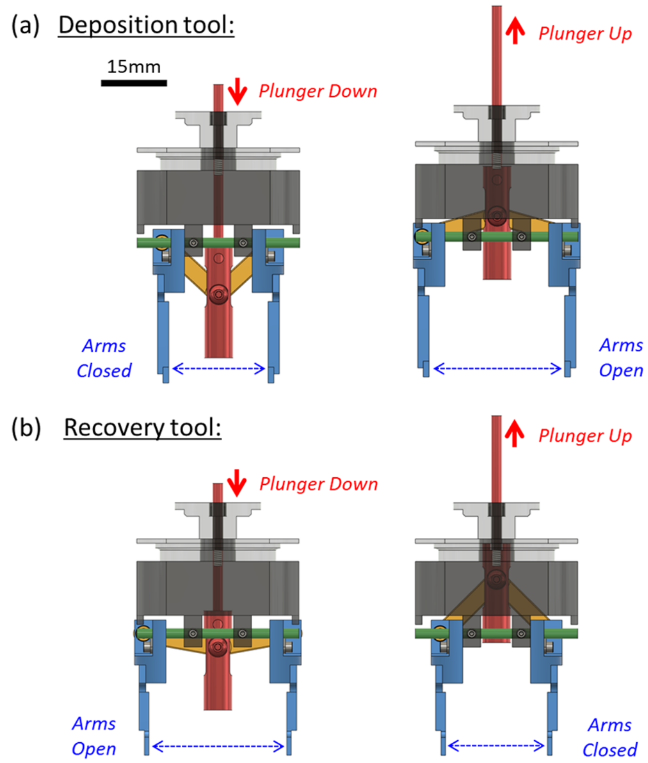

FIG. 4. Tool arm and plunger positions for attachment to STM head. (a) Deposition tool shown from front view with the plunger and arms at two positions: (Position 1) Arms closed and plunger down: starting position of deposition tool for transferring STM head. (Position 2) Arms open and plunger up: final position after depositing the STM. For clarity, the tool's body, groove, and button top are made transparent. (b) Recovery tool shown from front view with the plunger and arms at two positions: (Position 1) Arms open and plunger down: starting position to recover the STM head. (Position 2) Arms closed and plunger up: final position after recovering the STM head.

When the force applied to the plunger is sufficient to overcome the springs, the plunger moves in the direction of the force and causes the two arms to either open or close (Fig. 4). At the beginning of the deposition and recovery process, both tools have their plungers in the down position. Each tool is triggered during two events throughout the transfer process. The *first event* is when the STM head is connected to the LT plug. This occurs because the bottom of the plunger sits on top of the STM head as the tool and counterbalance are lowered further. The gravitational weight of the tool and counterbalance overcomes the compression spring force of the tool, allowing the plunger to move to the up position. For the deposition tool, this opens the arms and disconnects it from the STM head. For the recovery tool, this closes the arms and connects it to the STM head. The *second tool-triggering event* takes place within the vacuum chamber after the tool plungers have been triggered to the up position. The triggered tool and counterbalance are raised to the terminal post, which passes through a hole in the center of the counterbalance to engage with the top of the tool plunger and move it down. This closes the arms of the deposition tool and opens the arms of the recovery tool, setting them back to their initial positions for a new transfer. After this second triggering event, the tools are transferred to the carousel for storage. The full details of the transfer process are covered in the Operation section.

IV. TOOL SELECTOR, FLEXIBLE WINCH-BASED MECHANISM, AND CAROUSEL

The winch-based pulley provides the vertical movement of the STM head and tools between the RT chamber and LT connector plug within the magnet (Fig. 2). The pulley drives the movement of the counterbalance, which attaches to the top of the tool via a tool selector.

A. Tool selector

A tool selector module, shaped as a slotted opening with a depressed circular inset in the center for holding tools, is built into the bottom of the pulley's counterbalance [Figs. 5(a)–5(c)]. The tool button tops interlock with the tool selector's circular inset, joining them together and allowing the counterbalance to support the tool. The cavity is open on the front and back so that tools held on the carousel can be rotated into and out of the tool selector.

The counterbalance has two slots along its outer diameter [Fig. 5(a)] through which the guide rails are inserted to control their travel path. A vertical through-hole passes through the center of the counterbalance [Fig. 5(b)] and is used to allow the terminal post access to the top of the tool plunger for triggering in the chamber.

The counterbalance serves as a constant weight (245 g) to the pulley drum and is made of 304 SS. The top of the counterbalance connects to the pulley drum via two wires. The wires are anchored in place with clamps and screws. The two wires and guide rails are rotated 90° from each other to keep the counterbalance level and prevent it from rotating out of place.

B. Winch-based mechanism and flexible wires

The winch-based mechanism enables the compact design of the transfer system. The pulley drum (304 SS) is supported by a shaft running through two ball bearings[42] [Fig. 5(a)] that are anchored to the vacuum chamber via two ports [Fig. 2(b)]. Its rotation is controlled by a motor that connects to the drum's support beam. The motor is driven with a controller that is operated using LabVIEW and a handheld device. The pulley drum has two parallel tracks along its outer diameter to accommodate two wires that wrap around the drum and attach to the top of the counterbalance [Figs. 5(d) and 5(e)].

To keep the flexible wires strong and to prevent breakage during operation, each wire is made of three thin NiCr wires[43] twisted

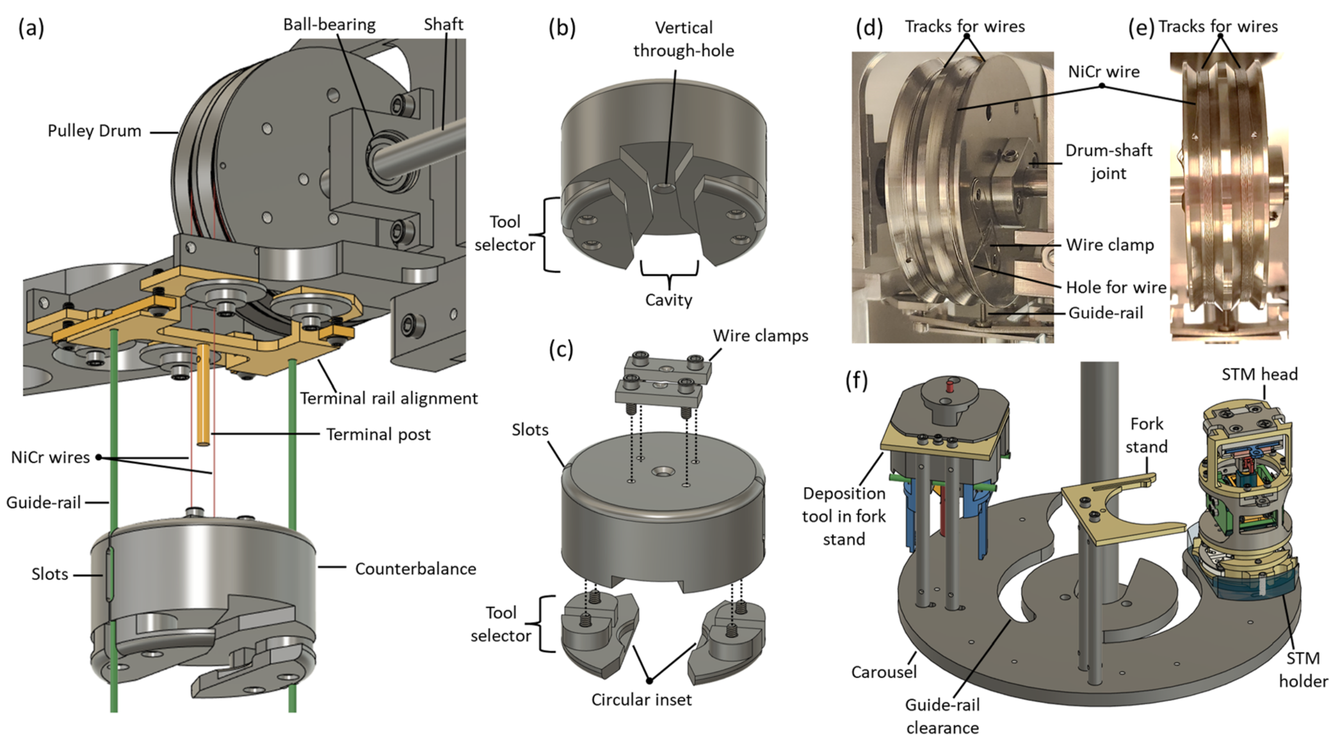

FIG. 5. Winch-based mechanism, tool selector, and carousel. (a) Schematic of pulley assembly showing the drum, counterbalance, and terminal (yellow). Vacuum chamber is removed for clarity. Two wires are shown connecting the pulley drum and counterbalance. The guide rails attach to the terminal and are held in place with nuts. (b) Schematic of the counterbalance showing the vertical through-hole and the tool selector cavity. (c) Exploded-view schematic of counterbalance showing the pulley wire clamps, slots for guide rails, and tool selector circular inset. (d) Photograph of the pulley drum showing the wire attachment clamp and wire wrapping around the drum. (e) Photograph of pulley drum from front view showing tracks and wire wrapping. (f) Carousel depicting fork stands and STM holder. The deposition tool is shown in the stand being held by its puck-style groove, and the recovery tool stand is shown without the tool.

together. The wire material and twisting were chosen to reduce the springiness of the wires. This is critical to prevent the wires from springing off the pulley drum when the counterbalance is supported and the wires are no longer under tension. Each wire is wrapped around one of the drum's outer diameter tracks and then passed through a hole to be anchored to either side of the drum with a clamp [Figs. 5(d) and 5(e)]. The clamps are fixed to the drum with screws and the wire is wrapped around the clamp to anchor it securely to the drum. Each track in the drum is flat at its center to allow single-layer wire wrapping, and angled side walls are used for wire guidance [Fig. 5(d)].

C. Terminal and rails

A terminal mounted to the support structure beneath the drum [Fig. 5(a)] separates the drum and counterbalance. Its role is to support the guide rails and to interact with the top of the tool's plunger. Cutouts in the terminal allow clearance for the two pulley wires to pass through the structure. Mounted to the center of the terminal is a post that protrudes downward toward the counterbalance, where it is able to pass through the counterbalance to the tool plunger. The terminal post is used to apply force to the tool's plunger and cause the tool arms to reset after a transfer.

The two guide rails are anchored at the terminal and at the bottom of the UHV insert. They are Teflon-coated stainless steel rods,[41] a material chosen to reduce friction during travel. Each end of the guide rail is threaded for mounting. At the bottom of the UHV insert, the guide rails are threaded into a ring mount attached to the LT connector plug to fix them in place [Fig. 2(c)]. The top end of the guide rail is secured to the terminal via a nut [Fig. 3(b)]. Alignment of the guide rails is crucial for ensuring smooth travel of the counterbalance between the vacuum chamber and the plug at the LT site. The terminal position is adjustable in-plane to align the guide rails with the UHV insert, and the nut holding the guide rails to the terminal controls the rail tension.

D. Carousel and storage of STM head and tools

The carousel in the chamber is used for storing the tools and STM head and for transferring them to the counterbalance

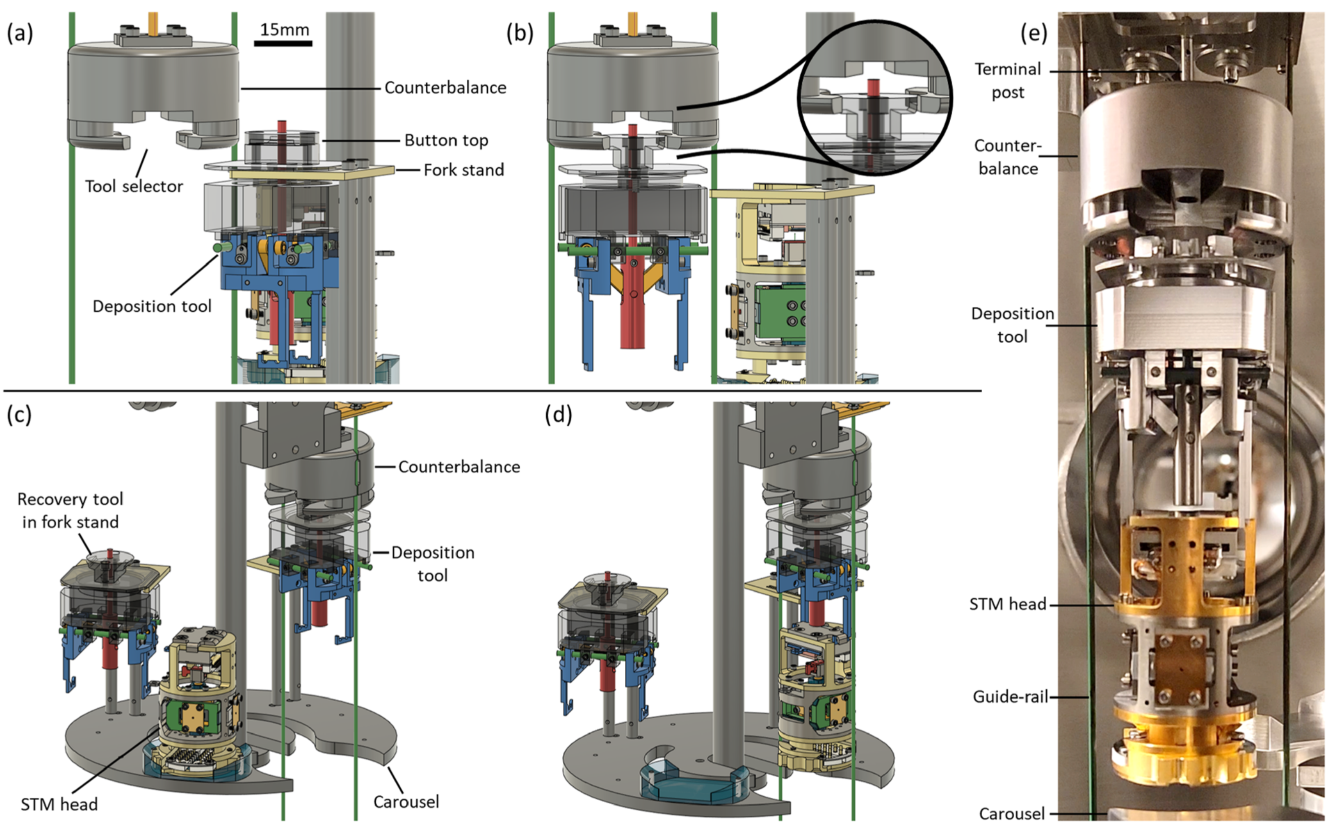

FIG. 6. Connection of STM head to transfer mechanism in RT chamber. (a) and (b) Schematics showing connection of the deposition tool to the counterbalance. (a) Starting position with deposition tool on carousel stand (arms closed/plunger down) and counterbalance empty. (b) Deposition tool placed in counterbalance tool selector. Carousel fork stand is rotated away from the tool. Inset shows interaction of tool selector and button top of the tool. (c) and (d) Schematics showing connection of the STM head to the deposition tool. (c) Starting position of the STM head in the carousel holder and the counterbalance holding the deposition tool. (d) Completed transfer assembly with counterbalance holding deposition tool and STM head. Carousel rotated to place opening below STM. (e) Photograph of transfer assembly within vacuum chamber before entering UHV insert.

[Fig. 2(b)]. Its vertical translation[44] (up to 50.8 mm) and rotation[45] (360°) are controlled via two stage manipulators located at the top of the vacuum chamber. Each tool is held by a fork stand via a puck-style interaction [Fig. 5(f)], leaving access to the button top of the tool. The STM head is stored on a shallow holder, leaving access to its top transfer handles. The carousel contains clearance holes through which the guide rails pass when the carousel is rotated. During a transfer, the counterbalance, tools, and STM pass through an opening in the carousel to enter the UHV insert.

V. OPERATION

A. Deposition of the STM within the LT magnet region

The transfer process begins with the deposition tool stored in the carousel fork stand with its arms closed and plunger down, and the counterbalance positioned near the terminal [Fig. 6(a)]. The deposition tool is transferred to the counterbalance by adjusting the height of the carousel until the tool's button top is at the height of the counterbalance's tool selector cavity. The tool enters the cavity by rotating and then lowering the carousel until the tool is supported by the circular inset in the tool selector. The fork stand is lowered further and then rotated away to disengage from the deposition tool, leaving the tool hanging below the counterbalance [Fig. 6(b)].

To transfer the STM head from the carousel to the tool [Fig. 6(c)], the carousel height is adjusted until the STM top transfer plate handles are between the height of the tool plunger and arms. The carousel is then rotated until the handles sit above the tool arm hooks. Lowering the carousel and STM head engages the handles and arm hooks, causing the STM head to be supported by the tool. The carousel is lowered further to disengage from the STM head and rotated until its opening is below the assembly [Figs. 6(d) and 6(e)]. The pulley drum is rotated to lower the counterbalance, deposition tool, and STM head through the carousel opening to the entrance of the UHV insert and down to the LT connector plug at the bottom of the UHV insert [Fig. 7(a)], following the path of the red arrow in Fig. 2(a).

Upon reaching the end of the insert, the weight of the counterbalance and deposition tool provides sufficient force to securely plug the STM head into the LT connector plug and make an electrical connection [Fig. 7(b)]. Since there is no optical access to monitor this process, the electrical lines of the system are measured (coarse and fine piezo motor lines), and a capacitance increase is observed when the STM is plugged into the LT connector. The counterbalance and deposition tool are lowered, further letting the tool plunger engage with the top of the stationary STM [Fig. 7(c)]. This applies a force to the bottom of the plunger, causing it to move up and the tool arms to open—disengaging the tool arms from the STM [Fig. 7(d)]. This action is verified by monitoring the tension of the drum wires within the chamber, which begin to slacken as the counterbalance is supported and indicate the tool triggering is complete [Fig. 7(e)]. An alignment mechanism installed on the top of the deposition tool ensures the proper alignment of the tool and counterbalance while triggering. It is described in the Appendix.

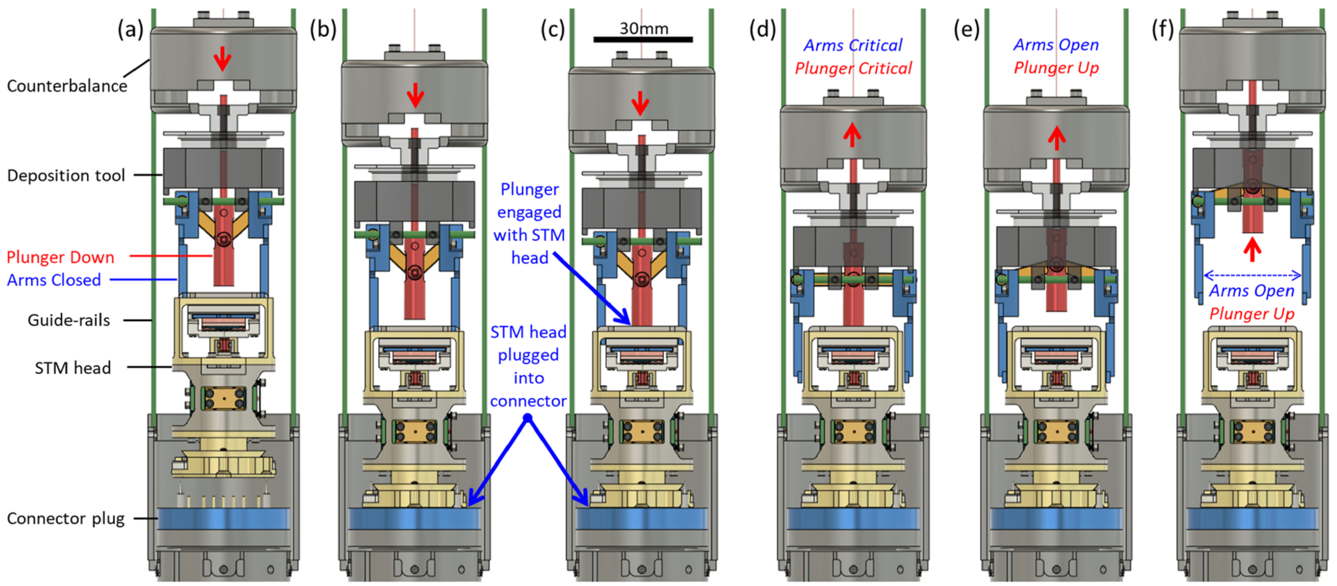

FIG. 7. Depositing the STM head at LT. Schematics do not show UHV insert and magnet for clarity. (a) Counterbalance, deposition tool, and STM head en route to LT connector plug (blue). Red arrow indicates position of tool plunger (down or up). (b) STM head connecting with LT connector plug. Counterbalance and deposition tool continue to be lowered. (c) Bottom of deposition tool plunger connecting with top of STM head transfer plate, beginning the trigger process where the plunger starts to move up and the arms start to open. (d) Critical point of the triggering process when the weight of the counterbalance and tool needs to overcome the tool spring force. Tool springs and arms are at their most extended position. (e) Triggering process complete with the tool plunger in the up position and the arms held open. Tool arms are clear of the STM head. Plunger top is hidden within the counterbalance through-hole. (f) Counterbalance and tool raised up to return it to the vacuum chamber. STM head is left plugged into the electrical connector and ready for experiments.

B. Resetting the tool in the chamber

The counterbalance and triggered deposition tool are raised [Fig. 7(f)] and returned to the RT chamber [Fig. 8(a)]. To trigger the tool plunger back to its original state, the terminal post is used. This is achieved by continuing to raise the counterbalance and tool and allowing the terminal post to enter the through-hole of the counterbalance and touch the top of the tool plunger [Fig. 8(b)]. The force of the terminal post causes the plunger to move down and the tool arms to return to the closed starting position [Figs. 8(c) and 8(d)]. The deposition tool is transferred back to the carousel by connecting the fork stand to the tool puck groove, using the carousel to raise the tool button top out of the counterbalance cavity inset, and then rotating the tool away from the counterbalance. The STM head remains on the LT plug at the bottom of the UHV insert for cooling and running experiments. This completes the transfer of the STM head to LT within the superconducting magnet.

The transfer process takes about 15 min, with most of that time consumed by travel within the UHV insert. In addition to transferring the STM to LT, we have utilized the winch-based mechanism to control the movement of a radiation baffle to provide a thermal radiation shield to the STM at LT. After the STM is positioned at LT and the deposition tool is transferred to the carousel, the counterbalance is connected to a radiation baffle in the chamber. The radiation baffle is moved into the UHV insert, where it lowers the base temperature of the STM. Its position within the UHV insert is a reliable method

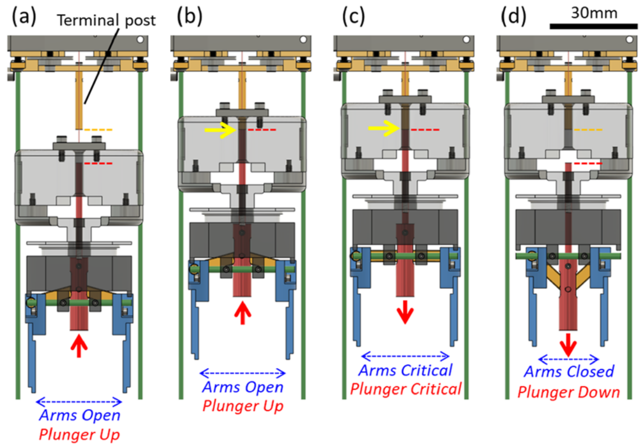

FIG. 8. Resetting the tool with the terminal post. The process is shown for the deposition tool in schematic form, but the recovery tool follows the same steps. For clarity, the top portion of the counterbalance is transparent in the images to see the tool plunger and terminal post interaction. (a) Counterbalance and deposition tool (arms open/plunger up) raised within the vacuum chamber. Red dashed line shows location of tool plunger top. Yellow dashed line shows location of terminal post end. (b) Terminal post entering counterbalance through-hole and starting to engage with top of tool plunger. Interaction indicated with yellow arrow. (c) Terminal post pushing the tool plunger down, causing it to move to the critical position. (d) Terminal post completes pushing the tool plunger to its down position, which closes the tool arms.

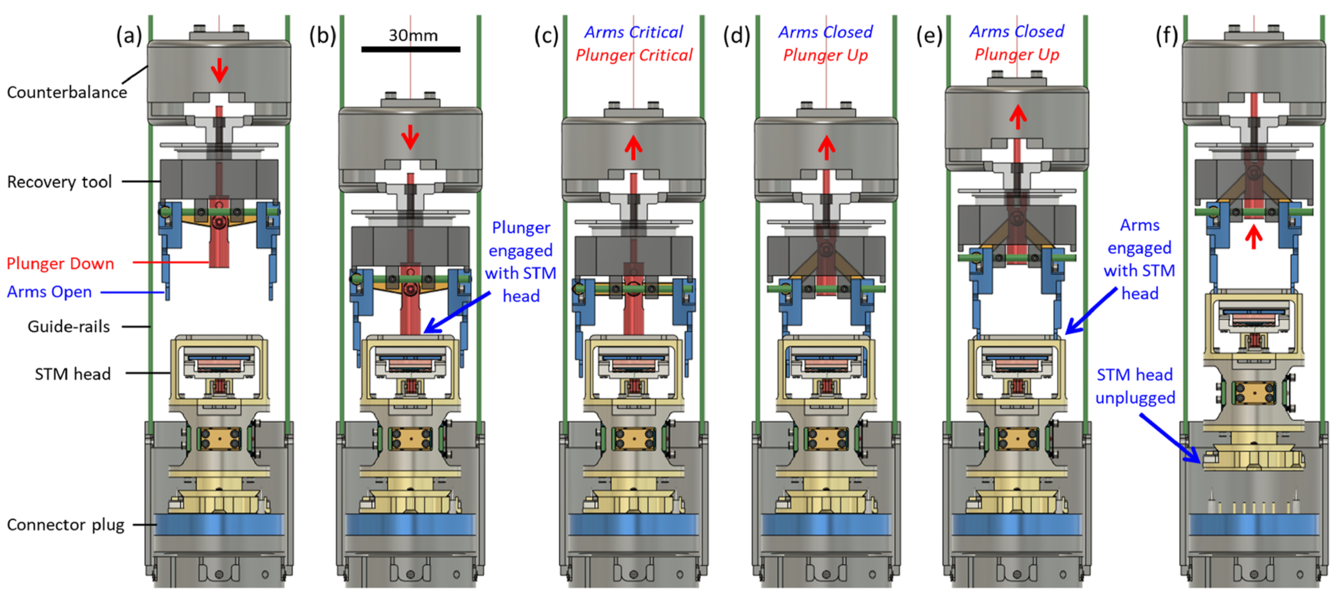

FIG. 9. Retrieval of the STM head from LT to return to RT. UHV insert and magnet not shown for clarity. (a) Counterbalance and recovery tool (arms open/plunger down) en route to STM head that is plugged into the LT connector within the UHV insert. Red arrow indicates position of tool plunger (down or up). (b) Recovery tool plunger engaging with top of STM head transfer plate, beginning triggering process where the plunger starts to move up and arms start to close. Counterbalance and recovery tool continue to be lowered. (c) Critical point of the triggering process where tool spring and arms are at their most extended. (d) Triggering process complete and tool plunger is moved to the up position and the arms are closed. Plunger top is hidden within the counterbalance vertical through-hole. (e) Counterbalance and recovery tool are raised up to allow the tool arms to engage with the STM head transfer plate handles. (f) Counterbalance, recovery tool, and STM head are raised up, which disconnects the STM head from the electrical connector plug and allows it to return to the vacuum chamber.

to gently vary the temperature of the STM head. The full details of the radiation baffle are previously published.[34]

C. Retrieval of the STM to return to RT

The recovery tool is transferred from the carousel fork stand to the counterbalance cavity insert following the same procedure as for the deposition tool [Figs. 6(a) and 6(b)]. The recovery tool arms begin in the open position, and the tool plunger is down. The carousel is rotated to allow the connected counterbalance and recovery tool to pass as they are lowered to the STM head at LT [Fig. 9(a)]. Because the tool arms are open, they will pass around the sides of the STM head. When the bottom of the recovery tool plunger interacts with the top of the STM head [Fig. 9(b)], the weight of the tool and counterbalance causes the plunger to move up and the tool arms to close [Figs. 9(c) and 9(d)]. This process is monitored by watching the tension of the pulley wire and is successful when the wires slacken.

Once the recovery tool arms are closed, the drum raises the counterbalance and recovery tool. While they are rising, the tool arms engage with the STM top handles [Fig. 9(e)] and unplug the STM head from the LT plug [Fig. 9(f)]. Once returned to the vacuum chamber, the STM head is transferred back to the carousel holder. To do this, the holder is rotated under the STM head and raised until the STM is supported and disengaged from the recovery tool arms. Then the STM head is rotated away from the tool by the carousel. The recovery tool plunger is triggered to the down position by the terminal post, resetting the tool arms to the open position. The tool is then transferred back to the carousel fork stand following the same methods as used with the deposition tool. This completes the STM head recovery process to RT.

VI. SUMMARY

We have described the design and operation of a novel low-profile internally mounted vertical transfer mechanism,[31–33] implemented within a cryogen-free UHV platform with a superconducting magnet.[34] This compact design is made possible by the use of a flexible winch-based mechanism, gravity-assisted attachment tools, and a low-force electrical connector. The transfer mechanism reliably transports a modular quick-connect STM head between RT and LT stations and plugs it into an LT electrical connector. Through the use of collapsible components, we have substantially reduced the size of the transfer mechanism, while at the same time diminishing susceptibility to vibrational noise and simplifying alignment within the cryostat bore. Furthermore, by eliminating excess pumping volume and the need for high ceilings, this design enables implementation in standard laboratories and broadens the access of LT STM to studies of μm-sized samples. The versatile transfer method described here is suitable for a variety of applications requiring transporting tools, samples, and radiation baffles[34] into small spaces with limited optical access.

ACKNOWLEDGMENTS

The authors thank the following for helpful discussions and/or technical assistance: Paul Pickard, William Schneider, Eric Paduch, and Cole Woloszyn from the Rutgers Physics and Astronomy Machine Shop. The instrumentation and infrastructure were primarily supported by Nos. DOE-FG02-99ER45742, NSF-MRI 1337871, and Gordon and Betty Moore Foundation No. GBMF9453.

AUTHOR DECLARATIONS

Conflict of Interest

The authors have no conflicts to disclose.

Author Contributions

Angela M. Coe: Conceptualization (equal); Data curation (equal); Formal analysis (equal); Investigation (equal); Methodology (equal); Writing – original draft (equal). **Guohong Li**: Conceptualization (equal); Investigation (equal); Methodology (equal); Supervision (equal); Writing – review & editing (equal). **Eva Y. Andrei**: Conceptualization (equal); Funding acquisition (lead); Investigation (equal); Project administration (equal); Resources (equal); Supervision (equal); Validation (equal); Writing – review & editing (equal).

A.M.C., G.L., and E.Y.A. have Patent No. US 11,474,127 B2 issued. A.M.C., G.L. and E.Y.A. have Patent No. US 12,098,026 B2 issued and WO 2019/209592 A2 pending. A.M.C., G.L., and E.Y.A. have Patent No. WO 2021/226354 A1 pending. A.M.C., G.L., and E.Y.A. have Patent Application No. US 63/691,509 pending. A.M.C., G.L., and E.Y.A. have Patent Application No. US 18/810,045 pending.

DATA AVAILABILITY

The data that support the findings of this study are available from the corresponding author upon reasonable request.

APPENDIX: TOOL DIFFERENCE AND TOOL ALIGNMENT HEIGHT LOCK MECHANISM

The design of the deposition and recovery tools is similar with four key differences enabling their opposite arm operations for a given plunger position (Fig. 4). The most important difference is the joint position of the plunger pivot beams. For the recovery tool, this joint is higher than the deposition tool. The pivot beam length is kept the same for both tools (21 mm), so this causes the recovery arms to start in an open position. The pivot beam joint position impacts the length of the tool arms and plunger. The deposition tool arm length (24 mm) and plunger length (58 mm) are longer than the recovery tool arms (20 mm) and plunger (50 mm). The final minor tool difference is that the recovery tool arm hook is slightly larger to aid in attachment to the STM head in the LT region without optical access.

To ensure the deposition tool plunger is aligned to the counterbalance through-hole when triggering on the top of the STM head, a safety alignment height lock mechanism was installed on the tool [Figs. 10(a) and 10(b)]. The deposition tool has a larger spring-force to overcome to move the plunger to the up position. If the springs selected are too stiff, the weight of the tool alone will not be able to extend the springs. This means the combined weight of the tool and the counterbalance is needed to trigger the tool plunger. To ensure

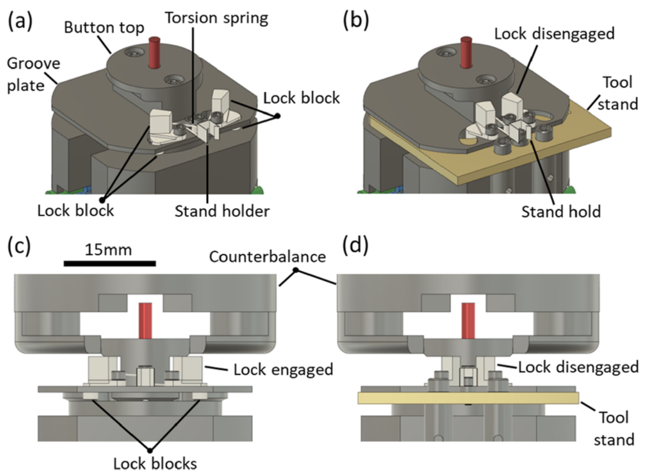

FIG. 10. Schematic of the deposition tool height lock mechanism. (a) Height lock located on the back of deposition tool groove plate. Shown with the lock engaged (torsion spring extended). (b) Fork stand shown holding the deposition tool and disengaging the height lock. Fork stand contacts the lock blocks extending below the groove plate and collapses the torsion spring by rotating the lock blocks inwards and holding them closed. The lock's stand holder is connected to a post on top of the fork stand to fix the position. (c) Deposition tool held by counterbalance with the height lock engaged. This arrangement is used during the vertical transfer process when depositing the STM head. (d) Fork stand holding deposition tool while the tool is in the counterbalance showing the height lock disengaging. This arrangement is used to move the tool between the fork stand and the counterbalance.

the tool remains aligned to the counterbalance, a height lock mechanism is installed on the deposition tool to engage with the underside of the counterbalance. This height lock reduces the allowed travel between the tool and counterbalance from 4.3 to 0.5 mm. Without a height lock, the tool movement can cause the top of the plunger to miss entering the counterbalance through-hole, preventing the tool from triggering. The height lock forces the tool to remain aligned with the counterbalance and guarantees that the trigger will be successful. It is composed simply of two blocks mounted to the top of the deposition tool's groove plate. The two blocks are allowed to rotate about pivot joints and are linked together through a torsion spring. A portion of the blocks extends below the tool groove plate to interact with the carousel fork stand; this is used to control the lock engagement. When the deposition tool is not held by the fork stand, the height lock is engaged [Fig. 10(c)]. This expands the torsion spring, allowing the top of the height lock to sit 0.5 mm below the bottom of the counterbalance. When the fork stand holds the deposition tool, the height lock is automatically disengaged [Fig. 10(d)]. This is achieved by the fork rotating the blocks and collapsing the torsion spring, which removes the height restriction imposed by the lock and allows the tool to be transferred between the fork stand and counterbalance. The deposition tool has an additional stand holder to ensure the height lock remains disengaged while held within the fork stand. The height lock engagement and disengagement occur automatically during a vertical transfer process without any additional steps. The recovery tool does not require a height lock because the spring force is weaker, and the weight of the recovery tool alone can trigger its plunger.

REFERENCES

[1] G. Binnig, H. Rohrer, C. Gerber, and E. Weibel, "Surface studies by scanning tunneling microscopy," Phys. Rev. Lett. **49**(1), 57–61 (1982).

[2] G. Binnig, H. Rohrer, C. Gerber, and E. Weibel, "Tunneling through a controllable vacuum gap," Appl. Phys. Lett. **40**(2), 178–180 (1982).

[3] G. Binnig and H. Rohrer, "Scanning tunneling microscopy—From birth to adolescence," Rev. Mod. Phys. **59**(3), 615–625 (1987).

[4] K. Hashimoto, C. Sohrmann, J. Wiebe, T. Inaoka, F. Meier, Y. Hirayama, R. A. Römer, R. Wiesendanger, and M. Morgenstern, "Quantum Hall transition in real space: From localized to extended states," Phys. Rev. Lett. **101**(25), 256802 (2008).

[5] Ø. Fischer, M. Kugler, I. Maggio-Aprile, C. Berthod, and C. Renner, "Scanning tunneling spectroscopy of high-temperature superconductors," Rev. Mod. Phys. **79**(1), 353–419 (2007).

[6] A. L. de Lozanne, S. A. Elrod, and C. F. Quate, "Spatial variations in the superconductivity of Nb_3Sn measured by low-temperature tunneling microscopy," Phys. Rev. Lett. **54**(22), 2433–2436 (1985).

[7] G. Li and E. Y. Andrei, "Observation of Landau levels of Dirac fermions in graphite," Nat. Phys. **3**(9), 623–627 (2007).

[8] G. Li, A. Luican, and E. Y. Andrei, "Scanning tunneling spectroscopy of graphene on graphite," Phys. Rev. Lett. **102**(17), 176804 (2009).

[9] A. Luican, G. Li, and E. Y. Andrei, "Quantized Landau level spectrum and its density dependence in graphene," Phys. Rev. B **83**(4), 041405 (2011).

[10] R. Wiesendanger, "Spin mapping at the nanoscale and atomic scale," Rev. Mod. Phys. **81**(4), 1495–1550 (2009).

[11] W. Meng *et al.*, "Atomically resolved probe-type scanning tunnelling microscope for use in harsh vibrational cryogen-free superconducting magnet," Ultramicroscopy **205**, 20–26 (2019).

[12] C.-P. Lu, G. Li, J. Mao, L.-M. Wang, and E. Y. Andrei, "Mid-gap states, and gating effects in MoS_2," Nano Lett. **14**(8), 4628–4633 (2014).

[13] C.-P. Lu, G. Li, K. Watanabe, T. Taniguchi, and E. Y. Andrei, "MoS_2: Choice substrate for accessing and tuning the electronic properties of graphene," Phys. Rev. Lett. **113**(15), 156804 (2014).

[14] S. H. Tessmer, D. J. V. Harlingen, and J. W. Lyding, "Integrated cryogenic scanning tunneling microscopy and sample preparation system," Rev. Sci. Instrum. **65**(9), 2855–2859 (1994).

[15] PanScan Freedom—Tesla, RHK Technology, Inc., Troy, Michigan.

[16] T. Esat, P. Borgens, X. Yang, P. Coenen, V. Cherepanov, A. Raccanelli, F. S. Tautz, and R. Temirov, "A millikelvin scanning tunneling microscope in ultra-high vacuum with adiabatic demagnetization refrigeration," Rev. Sci. Instrum. **92**(6) (2021).

[17] M. Kugler, C. Renner, Ø. Fischer, V. Mikheev, and G. Batey, "A ^{3}He refrigerated scanning tunneling microscope in high magnetic fields and ultrahigh vacuum," Rev. Sci. Instrum. **71**(3), 1475–1478 (2000).

[18] S. Misra, B. B. Zhou, I. K. Drozdov, J. Seo, L. Urban, A. Gyenis, S. C. J. Kingsley, H. Jones, and A. Yazdani, "Design and performance of an ultra-high vacuum scanning tunneling microscope operating at dilution refrigerator temperatures and high magnetic fields," Rev. Sci. Instrum. **84**(10), 103903 (2013).

[19] T. Balashov, M. Meyer, and W. Wulfhekel, "A compact ultrahigh vacuum scanning tunneling microscope with dilution refrigeration," Rev. Sci. Instrum. **89**(11), 113707 (2018).

[20] S. H. Pan, E. W. Hudson, and J. C. Davis, "^{3}He refrigerator based very low temperature scanning tunneling microscope," Rev. Sci. Instrum. **70**(2), 1459–1463 (1999).

[21] T. Machida, Y. Kohsaka, and T. Hanaguri, "A scanning tunneling microscope for spectroscopic imaging below 90 mK in magnetic fields up to 17.5 T," Rev. Sci. Instrum. **89**(9), 093707 (2018).

[22] P.-F. Chung *et al.*, "Design and performance of an ultrahigh vacuum spectroscopic-imaging scanning tunneling microscope with a hybrid vibration isolation system," Rev. Sci. Instrum. **95**(3) (2024).

[23] USM1300 Low Temperature UHV STM, UNISOKU Co., LDT, Osaka, Japan.

[24] A. M. Coe, G. Li, and E. Y. Andrei, "Modular scanning probe microscope head," Patent. Pub. No.: US 11,474,127 B2. Application No.: 17/313,743 (May 6, 2021).

[25]A. M. Coe, G. Li, and E. Y. Andrei, "Quick-connect scanning tunneling microscope head with nested piezoelectric coarse walkers," Rev. Sci. Instrum. **95**(7), 073703 (2024).
[26]Y. J. Song, A. F. Otte, V. Shvarts, Z. Zhao, Y. Kuk, S. R. Blankenship, A. Band, F. M. Hess, and J. A. Stroscio, "Invited review article: A 10 mK scanning probe microscopy facility," Rev. Sci. Instrum. **81**(12), 121101 (2010).
[27]R. J. Celotta, S. B. Balakirsky, A. P. Fein, F. M. Hess, G. M. Rutter, and J. A. Stroscio, "Invited Article: Autonomous assembly of atomically perfect nanostructures using a scanning tunneling microscope," Rev. Sci. Instrum. **85**(12), 121301 (2014).
[28]J. Schwenk *et al.*, "Achieving μeV tunneling resolution in an in-operando scanning tunneling microscopy, atomic force microscopy, and magnetotransport system for quantum materials research," Rev. Sci. Instrum. **91**(7), 071101 (2020).
[29]D. Wong, S. Jeon, K. P. Nuckolls, M. Oh, S. C. J. Kingsley, and A. Yazdani, "A modular ultra-high vacuum millikelvin scanning tunneling microscope," Rev. Sci. Instrum. **91**(2), 023703 (2020).
[30]G. Li, A. Luican, and E. Y. Andrei, "Self-navigation of a scanning tunneling microscope tip toward a micron-sized graphene sample," Rev. Sci. Instrum. **82**(7), 073701 (2011).
[31]A. M. Coe, G. Li, and E. Y. Andrei, "Low profile transfer mechanism for controlled environments," Patent. Pub. No.: WO 2019/209592 A2. Application No.: PCT/US2019/027929 (April 17, 2019).
[32]A. M. Coe, G. Li, and E. Y. Andrei, "Low profile transfer mechanism for controlled environments—Divisional," Patent. U.S. Provisional Application 18/810,045 (August 20, 2024).
[33]A. M. Coe, G. Li, and E. Y. Andrei, "Tool changes for a low-profile transfer mechanism," Patent. U.S. Provisional Application 63/691,509 (September 6, 2024).
[34]A. M. Coe, G. Li, and E. Y. Andrei, "Cryogen-free modular scanning tunneling microscope operating at 4-K in high magnetic field on a compact ultra-high vacuum platform," Rev. Sci. Instrum. **95**(8), 083702 (2024).
[35]Custom built vacuum chambers, Kurt J. Lesker, Jefferson Hills, Pennsylvania.
[36]Custom UHV Insert (316 stainless steel, inner diameter of 45.847 mm, 0.889 mm thick, 1.1 m in length), BellowsTech, Ormond Beach, Florida.
[37]Model 90-275-010LCF, Superconducting magnet solenoid; 9 T at 4.2 K; twisted multi-filamentary NbTi/Cu, Cryomagnetics, Inc., Oak Ridge, Tennessee.
[38]Model attoDRY1100, Closed-cycle cryogen free cryostat; top-loading design; 2″ bore size; base temperature 4 K; 9 T magnet, attocube systems AG, Munich, Germany.
[39]Model 1447360-8, C-Clip PCB Spring Contact, Gold plated BeCu, TE Connectivity, Berwyn, PA.
[40]CeramTec North America LLC, Laurens, SC.
[41]Model CGWX-0900-36, PTFE coated stainless steel 304 wire; 0.09" diameter; 36" long, Component Supply, Sparta, Tennessee.
[42]Model 68600, Radial Ball bearing, MDC Precision, Hayward, California.
[43]Model 8880K83, Nickel Chromium Alloy wire 0.008″ diameter, McMaster Carr, Aurora, Ohio.
[44]Model LSM38-50-H, Standard Travel Linear Shift Mechanism, Kurt J. Lesker, Jefferson Hills, Pennsylvania.
[45]Model MD40, MagiDrive Series Magnetically Coupled Rotary Motion Feedthrough, UHV Design, East Sussex, UK.
[46]A. M. Coe, G. Li, and E. Y. Andrei, "Damping base for modular scanning probe microscope head," Patent. Pub. No.: WO 2021/226354 A1, Application No.: PCT/US2021/031120 (May 6, 2021).